Heteroatom Chemistry
Volume 17, Number 3, 2006

Synthesis and Structure of the Coordinatively Unsaturated Boron Subphthalocyanine Cation, $[B(SubPc)]^+$

Tsuyoshi Kato,[1] Fook S. Tham,[1] Peter D. W. Boyd,[2]
and Christopher A. Reed[1]

[1] *Center for S and P Block Chemistry, Department of Chemistry, University of California, Riverside, CA 92521, USA*

[2] *Department of Chemistry, The University of Auckland, Private Bag 92019, Auckland, New Zealand*

Received 6 September 2005; revised 13 November 2005

ABSTRACT: *The boron subphthalocyanine cation, $B(SubPc)^+$, has been prepared as a salt of a weakly coordinating carborane anion, $CHB_{11}Me_5Br_6^-$, by a metathesis reaction of $Et_3Si(CHB_{11}Me_5Br_6)$ with B(SubPc)Cl. The separation of the cation and anion in the X-ray structure indicates coordinative unsaturation at the boron center, and this is corroborated by DFT calculations. A strongly Lewis acidic nature for the $B(SubPc)^+$ cation is indicated by its hydrolysis to an unusual product, the di-*meso-N-*protonated μ-oxo dimer, $[H(SubPc)B\text{-}O\text{-}B(SubPc)H]^{2+}$.* © 2006 Wiley Periodicals, Inc. Heteroatom Chem 17:209–216, 2006; Published online in Wiley InterScience (www.interscience.wiley.com). DOI 10.1002/hc.20223

INTRODUCTION

Coordination chemistry for boron with macrocyclic N-donor ligands has been developing in recent years [1–4]. Too small to fit as a single atom into traditional tetraazamacrocycles such as porphyrins or phthalocyanines, boron forms a stable complex with the triazamacrocycle, subphthalocyanine [5]. Indeed, the subphthalocyanine macrocycle is stable only when coordinated to boron, typically as the four-coordinate B(SubPc)Cl complex, **1**.

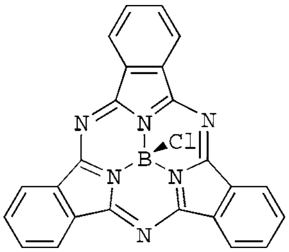

B(SubPc)Cl is important as an intermediate in the formation of unsymmetrical phthalocyanines by ring expansion with a diiminoisoindoline [6,7]. Upon formation of the phthalocyanine, the boron atom is no longer bound to the macrocycle. It has been proposed that the $B(SubPc)^+$ cation, formed by loss of chloride from **1**, precedes the ring expansion reaction [7]. We have therefore targeted the synthesis of this cation using a very weakly coordinating counterion. A carborane anion, $CHB_{11}Me_5Br_6^-$, was chosen because of its inertness toward reactive main group cations and its excellent crystallizing properties [8]. Tetraphenylborate is known to be unsuitable as a weakly coordinating anion since the phenyl derivative $(C_6H_5)B(SubPc)$ is formed when

---

Correspondence to: P. D. W. Boyd; e-mail: pdw.boyd@auckland.ac.nz. or C. A. Reed; email: chris.reed@ucr.edu

$[Bu_4N][B(C_6H_5)_4]$ is reacted with phthalonitrile [9].

Thus, we were interested in whether a “bare” $B(SubPc)^+$ borenium ion could be prepared and how strongly it would interact with the “least coordinating” anion [8]. Out-of-plane displacements of the central iron atom in iron porphyrin complexes have been used as a measure of the coordinating ability of axial ligands [10,11] so it was of interest whether a boron atom, in the naturally domed subphthalocyanine ligand, would respond similarly. Competition between coordinating anions and neutral N-atom donors has been studied in dialkylborenium-like species, $R_2BL(SO_3CF_3)$ [12]. The long-term goal of this work is to develop new Lewis acids based on borenium ions [13,14]. Boron subpthalocyanines are of current interest in the development of photo- and electro-active assemblies [15], and axial ligand changes may become an important part of the fine-tuning of their electronic properties.

RESULTS AND DISCUSSION

The abstraction of chloride ion from B(SubPc)Cl, **1**, to give $[B(SubPc)][CHB_{11}H_5Br_6]$, **2**, was achieved with triethylsilyl carborane in toluene (Eq. (1)). The color of the solution changes from bright magenta to deep purple.

$$B(SubPc)Cl + Et_3Si(CHB_{11}Me_5Br_6) \rightarrow [B(SubPc)][CHB_{11}Me_5Br_6] + Et_3SiCl \quad (1)$$

Trialkylsilyl species with weakly coordinating anions are amongst the strongest halophilic electrophiles known [16]. Their use in this work is necessitated not by any particular difficulty in removing chloride from **1** but by the need to have a volatile byproduct. Ethyl groups on silicon were chosen to give good volatility to the trialkylsilyl chloride byproduct. The weaker halophilic reagent Ag(carborane) achieves metathesis, but the separation of the insoluble AgCl and the poorly soluble **2** is problematic. ^1H NMR showed good purity, and the resonances show an expected downfield shift relative to **1**. The solubility is too low for ^{13}C NMR spectroscopy, and a ^{11}B NMR signal for the cation was unobservable, presumably due to large quadrupolar broadening in the anisotropic environment of the cation. A signal has been observed for the more nearly isotropic **1** at ca. −18 ppm [9] and is calculated from DFT calculations (B3LYP/6-31G(d)//B3LYP/6-311+G(2d,p) at ca. −18.6 ppm (anisotropy 0.50). For the $[B(SubPc)]^+$ cation in **2**, the ^{11}B signal is calculated to be at +7.4 ppm (anisotropy 0.82).

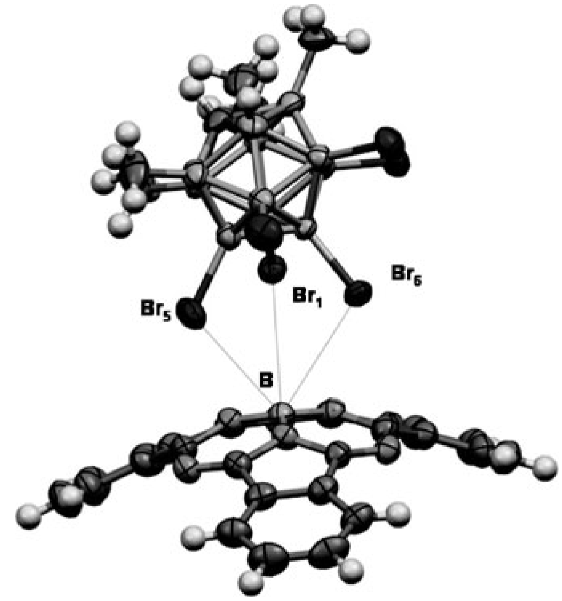

FIGURE 1 Cation/anion relationship in the crystal structure of $[B(SubPc)][CHB_{11}Me_5Br_6]\cdot 1.25C_6H_4Cl_2$, **2**. Thermal ellipsoids probability level 50%.

Single crystals of **2** suitable for X-ray crystal structure determination were grown from *o*-dichlorobenzene.

As shown in Fig. 1, the cation and anion have a commensurate pairing relationship with approximate three-fold symmetry, the aza-bridging N atoms of the macrocycle having an eclipsed arrangement with a triangular face of Br atoms (Br_1, Br_5, Br_6) from the carborane.

As shown in Fig. 2, these cation/anion pairs are well separated from each other in the lattice by *o*-dichlorobenzene solvate molecules which fill a cavity created by the face-to-face relationship of two domed SubPc cations.

As shown in Fig. 3, benzene moieties at the periphery of each SubPc molecule have π–π interactions with three neighboring SubPc units. The C···C contacts range from 3.39 to 3.52 Å. This type of overlap can be found in many structures of SubPc derivatives [9,17–21].

The relationship of the carborane anion to the SubPc cation (Fig. 1) is different from that observed with most main group element cations. In tightly ion-paired structures where there is some covalence in the element–halogen bonding, such as in R_3Si(carborane) [16], a single halogen atom interacts with the cationic center. In Et_2Al(carborane) [22,23] and in some silver salts of carboranes [24], *two* close element–halogen contacts are observed. The occurrence of *three* nearest neighbor interactions in the present structure suggests an essentially pure electrostatic relationship

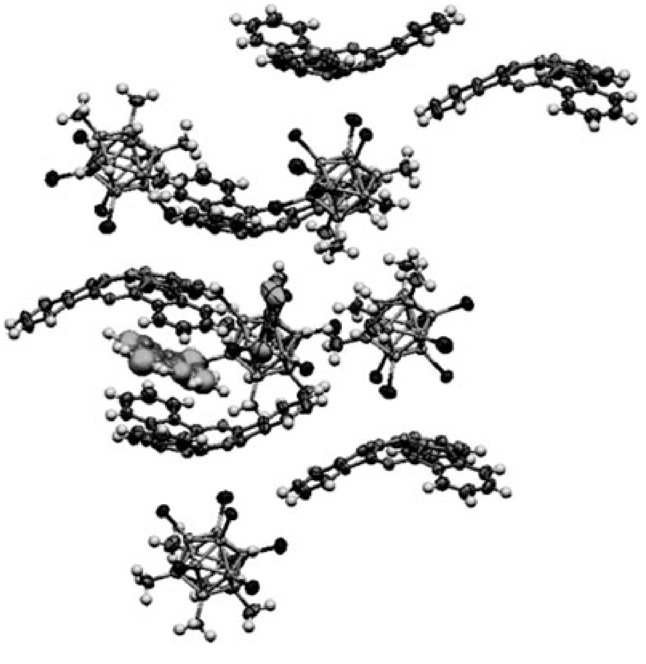

FIGURE 2 Packing of cations, anions, and solvent molecules in **2**. Thermal ellipsoids probability level 50%.

between the cation and anion where crystal-packing forces will control the orientation of the anion. This is supported by the long interion distances (B···Br = 3.59, 3.63, and 3.78 Å; Br···N = 3.63, 3.72, and 3.74 Å), arguably equal to the sum of the van der Waals radii (B ~ 1.7, N 1.55, Br 1.8–2.0 Å) [25].

The gas phase molecular structure of the $[B(SubPc)]^+$ cation has been calculated with and without carborane ion-pairing using density functional theory. The computed structures are compared to that obtained by X-ray diffraction in Table 1. The calculated structures show good agreement in bond lengths and angles as well as in the degree of doming of the macrocycle, as measured by displacements from the 3N plane of the coordinating nitrogen atoms. This corroborates the conclusion that the cation and anion are essentially free ions, related to each other only by electrostatic ion pairing, and without significant covalence in the B···Br axial bonding. The negative Br atoms center over the delocalized positive charge on the $[B(SubPc)]^+$ cation.

A preliminary indication of the reactivity of the $B(SubPc)^+$ cation in **2** has been obtained in the serendipitous crystallization of its hydrolysis product from solutions that had come in contact with moisture. From an analysis of single crystals of the diprotonated *μ*-oxo dimer $[H(SubPc)B\text{-}O\text{-}B(SubPc)H][CHB_{11}Me_5Br_6]_2 \cdot 0.375$*o*-dichlorobenzene·3.875toluene, **3**, it is evident that

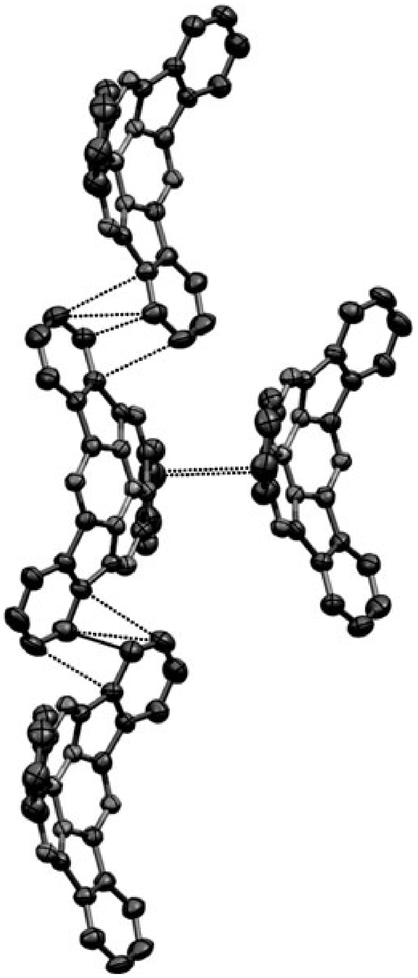

FIGURE 3 Arene–arene *π*–*π* interactions in the crystal structure of **2**. Thermal ellipsoids probability level 50%.

hydrolysis of **2** occurs according to Eq. (2).

$$2[B(SubPc)][CHB_{11}Me_5Br_6] + H_2O \rightarrow [H(SubPc)B\text{-}O\text{-}B(SubPc)H][CHB_{11}Me_5Br_6]_2 \quad (2)$$

Evidently, the $B(subPc)^+$ cation is a strong Lewis acid which reacts with H_2O to form a stable μ-oxo dimer, which is then protonated twice on an aza bridging N atom of each B(subPc) unit by the two equivalents of acid produced as the byproduct of hydrolysis. While protonation of the macrocycle was unanticipated and previously unknown, is nevertheless a logical outcome. Acid/base chemistry with μ-oxo dimers involving main group elements typically involves equilibria between hydroxo monomers and μ-oxo dimers [26]. Protonation of the bridging O atom in μ-oxo iron(III) porphyrin dimers is known [27,28], so the present result reflects the basicity of the aza bridge N atoms in the subPc macrocycle relative to the bridge O atom. The neutral μ-oxo dimer

TABLE 1 Selected Average Bond Lengths (Å), angles (°), and out of Plane Displacements for $[\text{B(SubPc)}]^+$ from the X-ray Structure of **2** and B3LYP/6-311G(d,p) Density Functional Theory Calculation, C_{3v} Symmetry

	*X-ray (**2**) [B(SubPcCl)]*	*DFT*		*X-ray (**2**) [B(SubPcCl)]*	*DFT*
B-N$_1$	1.380(14)[1.466]	1.383[1.488] *1.389*	N$_3$-B-N$_2$	118.0(10)[105.3]	118.5[105.1] *117.5*
N$_1$-C$_1$	1.386(13)[1.366]	1.388[1.368] *1.383*	δ_{oop}(B)	0.197[0.583]	0.168[0.595] *0.220*
C$_1$-N$_2$	1.340(13)[1.344]	1.340[1.338] *1.339*	δ_{oop}(N$_2$)	−0.549[−0.552]	−0.517[−0.555] *−0.531*
C$_1$-C$_2$	1.455(15)[1.461]	1.449[1.456] *1.452*	δ_{oop}(C$_1$)	−0.397[−0.416]	−0.378[−0.421] *−0.381*
C$_2$-C$_5$	1.387(15)[1.391]	1.396[1.395] *1.396*	δ_{oop}(C$_2$)	−0.876[−0.925]	−0.806[−0.952] *−0.818*
C$_2$-C$_3$	1.430(15)[1.415]	1.443[1.429] *1.439*	δ_{oop}(C$_5$)	−1.368[−1.443]]	−1.252[−1.491] *−1.261*
C$_5$-C$_6$	1.381(17)[1.370]	1.388[1.389] *1.388*	δ_{oop}(C$_6$)	−1.830[−1.890]	−1.673[−1.998] *−1.680*
C$_6$-C$_7$	1.380(18)[1.394]	1.407[1.406] *1.407*	B-Cl	–[1.864]	—[1.881]

Entries in square brackets are the corresponding values for [BSubPcCl], [18]. Entries in italics are the corresponding values in the $[\text{B(SubPc)}]^+$ $[\text{CHB}_{11}\text{Me}_5\text{Br}_6]^-$ ion pair. The numbering scheme for the $[\text{B(SubPc)}]^+$ cation is shown in the diagram below.

(*t*-BuSubPc)B-O-B(*t*-BuSubPc) has been previously isolated [7,29].

The structure of the cation in **3** is shown in Fig. 4. The two BSubPc moieties are joined by a non linear B–O–B bridge (137.2°). There is a close π–π approach of a pair of benzopyrrole groups with closest contacts for N···N of 2.982 Å and C···C of 3.287 Å. Two bridging aza atoms are protonated in each dimer leading to a dication $[\text{H(SubPc)B-O-B(SubPc)H}]^{2+}$. The C—N bond lengths in the BSubPc groups are lengthened when the N is protonated in comparison to those involving the neutral aza bridges ($\text{C—N(H}^+)_{\text{average}}$ 1.367 Å, $\text{C—N}_{\text{average}}$ 1.342 Å). A density functional calculation (B3LYP/6-31G(d)) of the molecular structure of $[\text{H(SubPc)B-O-B(SubPc)H}]^{2+}$ was in agreement with this observation (calculated $\text{C—N(H}^+)_{\text{average}}$ 1.375 Å, $\text{C—N}_{\text{average}}$ 1.339 Å). Each protonated N is hydrogen bonded to a Br atom of a $\text{CHB}_{11}\text{Me}_5\text{Br}_6$ anion (Table 2). Each $[\text{H(SubPc)B-O-B(SubPc)H}]^{2+}$ unit is separated from another by disordered toluene molecules encapsulated between adjacent units leading to a one-dimensional ribbon like arrangement of the cations. The $\text{CHB}_{11}\text{Me}_5\text{Br}_6$ anions surround this construct with hydrogen-bonding interactions to the protonated N atoms (Fig. 5).

EXPERIMENTAL

B(SubPc)Cl was obtained from Aldrich Chemicals, and $\text{Et}_3\text{Si(CHB}_{11}\text{Me}_5\text{Br}_6)$ [30] was prepared by literature methods. Solvents were purified and dried by standard methods [31]. All operations were performed in a Vacuum Atmospheres Corp. glove box under He (O_2, $\text{H}_2\text{O} < 0.5$ ppm).

Preparation of $[\text{B(SubPc)}][\text{CHB}_{11}\text{Me}_5\text{Br}_6]\cdot$ 1.25o-dichlorobenzene, **2**

B(SubPc)Cl (1.08 g, 2.5 mmol) and $\text{Et}_3\text{Si(CHB}_{11}\text{H}_5\text{Br}_6)$ (2 g, 2.5 mmol) were stirred overnight in *o*-dichlorobenzene (20 mL) in the absence of light. After removal of volatiles under vacuum, the product was precipitated in toluene as the dark purple product, which was collected by filtration and washed with hexanes (1.48 g, 55%). ^{1}H NMR (500 MHz, ODCB-D$_4$) $\delta = 0.63$ (s, 15H, CH$_3$), 0.20 (s, 1H, CH), 8.33 (m, 6H, CH$_{\text{Aromatic}}$), 9.27 (m, 6H, CH$_{\text{Aromatic}}$). Black single crystals of a 1.25 *o*-dichlorobenzene solvate were obtained by 1:1:1 successive layering of a saturated *o*-dichlorobenzene solution with toluene and hexanes in the dark. When crystallizations are

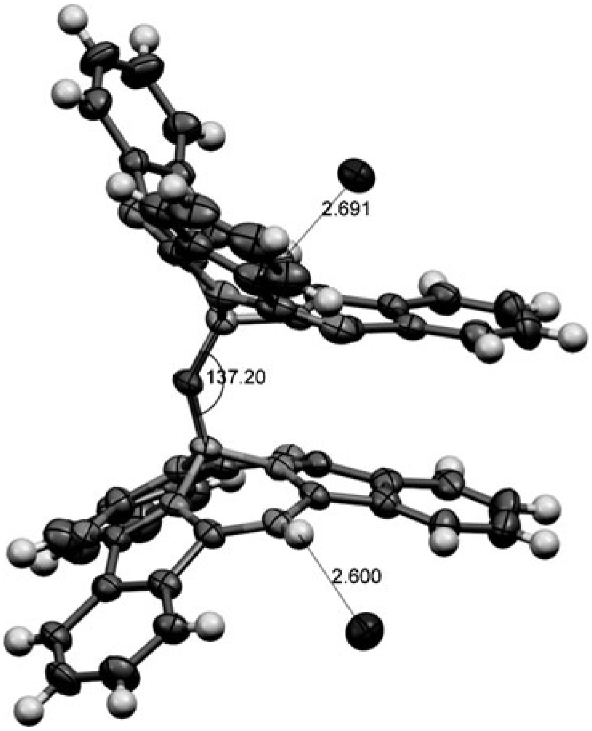

FIGURE 4 X-ray structure of one of the diprotonated μ-oxo dimer cations in **3**. Hydrogen bond N–H···Br distances indicated. Thermal ellipsoids probability level 50%.

carried out in toluene/*o*-dichlorobenzene solutions that had come in contact with moisture, black single crystals of the diprotonated μ-oxo dimer cation, $[H(SubPc)B\text{-}O\text{-}B(SubPc)H][CHB_{11}Me_5Br_6]_2\cdot 0.375$*o*-dichlorobenzene·3.875toluene, **3**, were deposited.

X-Ray Structure Analyses

A black-colored fragment of a prism was used for the study of $[B(SubPc)][CHB_{11}Me_5Br_6]1.25$*o*-dichlorobenzene, **2** (sample cr101m), and a black fragment of a needle was used for the study of $[H(SubPc)BOB(SubPc)H][CHB_{11}Me_5Br_6]_2\cdot 0.375$*o*-dichlorobenzene·3.875toluene, **3** (sample cr81s). The crystals were coated with Paratone oil and mounted onto glass fibers. X-ray intensity data were collected at 223(2) K on a Bruker SMART 1000 platform-CCD X-ray diffractometer system (Mo-radiation, $\lambda = 0.71073$ Å, 50 KV/40 mA power). For **2** a total of 1321 frames were collected for a hemisphere of reflections (with scan width of 0.3° in ω and ϕ angles of 0°, 90°, 180°, and 0° for every 606, 435, 230, and 50 frames, respectively, 30 s/frame exposure time) whilst for **3** a total of 3030 frames were collected for a sphere of reflections (with scan width of 0.3° in ω, starting ω and 2θ angles of −28°, and ϕ angles of 0°, 90°, 120°, 180°, and 240° for every 606 frames, 60 s/frame exposure time). The frames were integrated using the Bruker SAINT software package [32] with a narrow-frame integration algorithm. Based on a monoclinic crystal system, the integrated frames yielded a total of 25,532 reflections at a maximum 2θ angle of 49.42° (0.85 Å resolution), of which 8493 were independent reflections ($R_{\text{int}} = 0.0480$, $R_{\text{sig}} = 0.0570$, redundancy = 3.0, completeness = 99.8%) and 5740

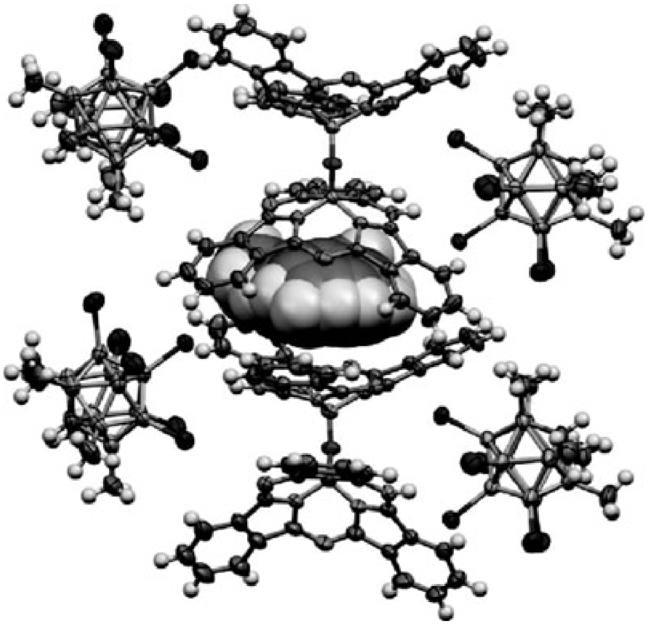

FIGURE 5 Packing arrangements of the cations and anions in $[H(SubPc)B\text{-}O\text{-}B(SubPc)H][CHB_{11}Me_5Br_6]_2\cdot 0.375$*o*-dichlorobenzene·3.875toluene, **3**. Thermal ellipsoids probability level 50%. Solvent molecules omitted for clarity except for space-filling model of disordered toluene between cations.

TABLE 2 Hydrogen Bonds in $[H(SubPc)BOB(SubPc)H][CHB_{11}Me_5Br_6]_2$, 3

D—H···A	*d(D—H) (Å)*	*d(H···A) (Å)*	*d(D···A) (Å)*	*<(DHA) (in deg)*
N(4′)—H(4′)···Br(6A)	0.87	2.69	3.445(6)	145.6
N(12′)—H(12′)···Br(6B)	0.87	2.60	3.345(7)	144.3
N(6″)—H(6″)···Br(6D)	0.87	2.58	3.334(7)	145.7
N(10″)—H(10″)···Br(6C)	0.87	2.60	3.328(7)	142.2

TABLE 3 Crystal Data and Structure Refinement for [B(SubPc)][$CHB_{11}Me_5Br_6$]1.25*o*-dichlorobenzene, **2** and [H(SubPc)B-O-B(SubPc)H][$CHB_{11}Me_5Br_6$]$_2$·0.375*o*-dichlorobenzene·3.875toluene, **3**

Identification code	cr101m	cr81s
Empirical formula	$C_{37.50}H_{33}B_{12}Br_6Cl_{2.50}N_6$	$C_{178.75}H_{181}B_{48}Br_{24}Cl_{1.50}N_{24}O_2$
Formula weight	1265.50	5187.37
Temperature (K)	223(2)	223(2)
Wavelength (Å)	0.71073	0.71073
Crystal system	Monoclinic	Monoclinic
Space group	*P*2(1)/n	*C*2/*c*
Unit cell dimensions	$a = 12.827(4)$ Å	$a = 86.77(4)$ Å
	$b = 19.415(6)$ Å	$b = 15.651(7)$ Å
	$c = 20.875(7)$ Å	$c = 35.777(15)$ Å
	$\beta = 106.223(6)^\circ$	$\beta = 100.024(8)^\circ$
Volume (Å^3)	4992(3)	47841(35)
Z	4	8
Density (calculated) (g cm^{-3})	1.684	1.440
Absorption coefficient (mm^{-1})	4.996	4.081
F(000)	2450	20344
Crystal size (mm^3)	0.21 × 0.19 × 0.10	0.35 × 0.17 × 0.09
Theta range for data coll.	1.46–24.71°	0.95–23.26°
Index ranges	$-12 \leq h \leq 15$, $-22 \leq k \leq 22$, $-24 \leq l \leq 24$	$-96 \leq h \leq 96$, $-17 \leq k \leq 17$, $-39 \leq l \leq 39$
Reflections collected	25,532	250,658
Independent reflections	8493 (*R*(int) = 0.0480)	34,371 (*R*(int) = 0.0748)
Completeness to θ	24.71° (99.8%)	23.26° (100.0%)
Absorption correction	Semiempir. from equivs	Semiempir. from equivs
Max. and min. transmission	0.6350 and 0.4201	0.7102 and 0.3293
Refinement method	Full-matrix least-square on F^2	Full-matrix least-square on F^2
Data/restraints/ parameters	8493/168/633	34371/1457/3080
Goodness-of-fit on F^2	1.017	1.085
Final *R* indices [$I > 2\sigma(I)$]	$R1 = 0.0465$, $wR2 = 0.1168$	$R1 = 0.0596$, $wR2 = 0.1852$
R indices (all data)	$R1 = 0.0802$, $wR2 = 0.1344$	$R1 = 0.0976$, $wR2 = 0.2123$
Largest difference in peak and hole (e.Å^{-3})	1.019 and −0.701	1.516 and −0.793

(67.6%) reflections were greater than $2\sigma(I)$ for **2**; whilst for **3** the integrated frames yielded a total of 250,658 reflections at a maximum 2θ angle of 46.52° (0.90 Å resolution), of which 34,371 were independent reflections ($R_{\mathrm{int}} = 0.0748$, $R_{\mathrm{sig}} = 0.0453$, redundancy = 7.3, completeness = 100%) and 23,105 (67.2%) reflections were greater than $2\sigma(I)$. Absorption corrections were applied to the raw intensity data using the SADABS programin the SAINT software. The Bruker SHELXTL (version 6.10) software package [33] was used for phase determination and structure refinement.

For 2, the distribution of intensities ($E^2 - 1 = 0.961$) and systematic absent reflections indicated one possible space group: *P*2(1)/*n*, later determined to be correct. Direct methods of phase determination followed by two Fourier cycles of refinement led to an electron density map from which most of the non-hydrogen atoms were identified in the asymmetric unit. With subsequent isotropic refinement, all of the non-hydrogen atoms were identified. There was one B(SubPc)$^+$ cation, one $CHB_{11}Me_5Br_6^-$ anion, and two partially occupied solvent molecules of $C_6H_4Cl_2$ present in the asymmetry unit. One $C_6H_4Cl_2$ was assigned 75% occupied, and the other disordered $C_6H_4Cl_2$ molecule was assigned a total of 50% occupied with 30%/20% disordered occupancy ratio. The disordered solvent molecule was refined with the atoms as isotropic displacement parameters. Atomic coordinates, isotropic and anisotropic displacement parameters of all the non-hydrogen atoms were refined by means of a full matrix least-squares procedure on F^2. The H-atoms were included in the refinement in calculated positions. The riding on the atoms to which they were attached. refinement converged at $R1 = 0.0465$, $wR2 = 0.1168$, with intensity, $I > 2\sigma(I)$.

For **3**, the distribution of intensities ($E^2 - 1 = 0.893$) and systematic absent reflections indicated two possible space groups, *C*2/*c* and *Cc*. The space group *C*2/*c* (#15) was later determined to be correct.

Direct methods of phase determination followed by two Fourier cycles of refinement led to an electron density map from which most of the non-hydrogen atoms were identified in the asymmetry unit of the unit cell. With subsequent isotropic refinement, all of the non-hydrogen atoms were identified. There were two $[H(SubPc)BOB(SubPc)H]^{2+}$ cations, four $CHB_{11}Me_5Br_6^-$ anions, three 25% occupied solvent molecules of *o*-dichlorobenzene, three fully occupied toluene, four 50% occupied C_6H_6, seven 25% occupied toluene, one 21% occupied toluene, and one 79% occupied toluene present in the asymmetric unit. The N—H bond length was fixed at 0.87 Å, and the H-atoms were located from the difference map.

A summary of the collection and refinement data is given in Table 3. Data have been deposited with the Cambridge Crystallographic Data Centre (www.ccdc.cam.ac.uk/conts/retrieving.html; 12 Union Rd, Cambridge CB2 1EZ, UK; fax: (44)1223-336-033; email: deposit@ccdc.cam.ac.uk) and can be obtained free of charge by quoting CCDC 281570 for **2** and CCDC 281569 for **3**. Figures were created using the Cambridge Crystallographic Database Mercury visualization software [34].

Calculations

Density functional calculations were carried out using the Gaussian 03 program [35]. Full geometry optimizations were carried out for the $[B(SubPc)]^+$ cation and the $[B(SubPc)][CHB_{11}Me_5Br_6]$ ion pair using the B3LYP density functional with the 6-311G(d,p) and 6-311+G(d) basis sets, respectively. Geometry optimizations for the larger $[H(SubPc)B\text{-}O\text{-}B(SubPc)H]^{2+}$ cation using a B3LYP/6-31G(d) model could not reproduce the π–π close contact between the two B(SubPc) moieties. The B-O-B angle calculated to be 139.8° which agreed well with the experimental value of 137.2° but the relative orientation of the [H(SubPc)B] groups was different. This may be due to either packing within the crystal or an incomplete description of the dispersive interactions required to account for π–π interactions. There was good agreement with the metric details within the $[H(SubPc)B]^+$ groups.

REFERENCES

[1] Senge, M. O. Angew Chem 1998, 37, 1071.
[2] Brothers, P. J. J. Porph Phthalo 2003, 6, 259.
[3] (a) Belcher, W. J.; Boyd, P. D. W.; Brothers, P. J.; Liddell, M. J.; Rickard, C. E. F. J Am Chem Soc 1994, 116, 8416; (b) Belcher, W. J.; Breede, M.; Brothers, P. J.; Rickard, C. E. F. Angew Chem 1998, 37, 1112; (c) Weiss, A.; Pritzkow, H.; Brothers, P. J.; Siebert, W. Angew Chem 2001, 40, 4182.
[4] Köhler, T.; Hodgson, M. C.; Seidel, D.; Veauthier, J. M.; Meyer, S.; Lynch, V.; Boyd, P. D. W.; Brothers, P. J.; Sessler, J. L. Chem Commun 2004, 1060.
[5] Claessens, C. G.; Gonzalez-Rodriguez, D.; Torres, T. Chem Rev 2002**,** 102, 835.
[6] Kobayashi, N.; Kondo, R.; Nakajima, S.; Osa, T. J Am Chem Soc 1990, 112, 9640.
[7] Kobayashi, N.; Ishizaki, T.; Ishii, K.; Konami, H. J Am Chem Soc 1999, 121, 9096.
[8] Reed, C. A. Acc Chem Res 1998, 31, 133.
[9] Potz, R.; Göldner, M.; Hückstädt, H.; Cornelissen, U.; Tutaß, A.; Homborg, H. Z Anorg Allg Chem 2000, 626, 588.
[10] Shelly, K.; Reed, C. A.; Y. J.; Scheidt, W. R. J Am Chem Soc 1986, 108, 3117.
[11] Evans, D. R.; Drovetskaya, T.; Bau, R.; Reed, C. A.; Boyd, P. D. W. J Am Chem Soc 1997, 119, 3633.
[12] Narula, C. K.; Nöth, H. Inorg Chem 1985, 24, 2532.
[13] Piers, W. E.; Bourke, S. C.; Conroy, K. D. Angew Chem 2005, 44, 5016.
[14] Kölle, P.; Nöth, H. Chem Rev 1985, 85, 399.
[15] Iglesias, R. S.; Claessens, C. G.; Torres, T.; Rahman, G. M. A.; Guldi, D. M. Chem Commun 2005, 2113 and references therein.
[16] Reed, C. A. Acc Chem Res 1998, 31, 325.
[17] Fukuda, T.; Olmstead, M. M.; Durfee, W. S.; Kobayashi, N. Chem Commun 2003 , 1256.
[18] Kietaibl, H. Monatsh Chem 1974 105, 405.
[19] Kasuga, K.; Idehara, T.; Handa, M.; Ueda, Y.;.Fujiwara, T.; Isa, K. Bull Chem Soc Jpn 1996, 69, 2559.
[20] Engel, M. K.; Yao, J.; Maki, H.; Takeuchi, H.; Yonehara, H.; Pac, C. Rep Kawamura Inst Chem Res 1997, 9, 53.
[21] Rauschnabel, J.; Hanack, M. Tetrahedron Lett 1995, 36, 1629.
[22] Kim, K-C.; Reed, C. A.; Long, G. S.; Sen, A. J Am Chem Soc 2002, 124, 7662.
[23] Pandey, K. K. Inorg Chem 1993, 42, 6764.
[24] Xie, Z.; Wu, B-M; Mak, T. C. W.; Manning, J.; Reed, C. A. J Chem Soc, Dalton Trans 1997, 1213.
[25] Bondi, A. J Phys Chem 1964, 68, 441.
[26] Yamamoto, Y., Akiba, K.-Y., Satoh, W., Nadano, R., Yamamoto, G. Chem Commun 1997, 1325.
[27] Scheidt, W. R., Cheng, B., Safo, M. K., Cukiernik, F., Marchon, J.-C., Debrunner, P. G. J Am Chem Soc 1992, 114, 4420.
[28] Evans, D. R.; Mathur, R. S.; Heerwegh, K.; Reed, C.A.; Xie, Z. Angew Chem, Int Ed 1997, 1335.
[29] Geyer, M.; Plenzig, F.; Rauschnabel, J.; Hanack, M.; del Rey, B.; Sastre, A.; Torres, T. Synthesis 1996, 1139.
[30] Stasko, D.; Reed, C. A. J Am Chem Soc 2002, 124, 1148.
[31] Perrin, D. D.; Armarego, W. L. F.; Perrin, D. R. Purification of Laboratory Chemicals; Pergamon Press: Sydney, 1980.
[32] SAINT Software Reference Manual, version 6.02A; Bruker Analytical X-Ray System, Inc.: Madison, WI, 1997–1998.
[33] SHELXTL Software Reference Manual, version 6.10; Bruker Analytical X-Ray System, Inc.: Madison, WI, Dec. 5, 2000.

[34] Bruno, I. J.; Cole, J. C.; Edgington, P. R.; Kessler, M.; Macrae, C. F.; McCabe, P.; Pearson, J.; Taylor, R. Acta Crystallogr 2002, 58, 389.

[35] Gaussian 03, Revision C.02; Frisch, M. J.; Trucks, G. W.; Schlegel, H. B.; Scuseria, G. E.; Robb, M. A.; Cheeseman, J. R.; Montgomery, J. A., Jr.; Vreven, T.; Kudin, K. N.; Burant, J. C.; Millam, J. M.; Iyengar, S. S.; Tomasi, J.; Barone, V.; Mennucci, B.; Cossi, M.; Scalmani, G.; Rega, N.; Petersson, G. A.; Nakatsuji, H.; Hada, M.; Ehara, M.; Toyota, K.; Fukuda, R.; Hasegawa, J.; Ishida, M.; Nakajima, T.; Honda, Y.; Kitao, O.; Nakai, H.; Klene, M.; Li, X.; Knox, J. E.; Hratchian, H. P.; Cross, J. B.; Bakken, V.; Adamo, C.; Jaramillo, J.; Gomperts, R.; Stratmann, R. E.; Yazyev, O.; Austin, A. J.; Cammi, R.; Pomelli, C.; Ochterski, J. W.; Ayala, P. Y.; Morokuma, K.; Voth, G. A.; Salvador, P.; Dannenberg, J. J.; Zakrzewski, V. G.; Dapprich, S.; Daniels, A. D.; Strain, M. C.; Farkas, O.; Malick, D. K.; Rabuck, A. D.; Raghavachari, K.; Foresman, J. B.; Ortiz, J. V.; Cui, Q.; Baboul, A. G.; Clifford, S.; Cioslowski, J.; Stefanov, B. B.; Liu, G.; Liashenko, A.; Piskorz, P.; Komaromi, I.; Martin, R. L.; Fox, D. J.; Keith, T.; Al-Laham, M. A.; Peng, C. Y.; Nanayakkara, A.; Challacombe, M.; Gill, P. M. W.; Johnson, B.; Chen, W.; Wong, M. W.; Gonzalez, C.; and Pople , J. A.; Gaussian, Inc., Wallingford CT, 2004.